J. Fluid Mech. (1966), *vol.* 26, *part* 4, *pp.* 689–715
Printed in Great Britain

The mechanism of entrainment in free turbulent flows

By A. A. TOWNSEND
Emmanuel College, Cambridge

(Received 27 January 1966)

A considerable quantity of observations and measurements exists concerning the phenomenon of intermittency which is connected closely with the entrainment process in free turbulent flows. A number of these are described in the first part of the paper and conclusions are drawn about the shape and motion of the bounding surface that separates turbulent and non-turbulent fluid. The salient features are that indentations of the surface grow and decay cyclically, that each cycle leads to substantial entrainment of ambient fluid into the turbulent region, that the indentations move at a considerable speed relative to the free stream, and that the surface has a comparatively simple form. The growth–decay cycle of the indentations suggests that a critical condition for growth exists, but the pressure field consequent on the convection velocity of the indentations makes for a Helmholtz type of instability that is unlikely to be stabilized by purely viscous behaviour of the turbulent fluid. It is known that the initial response of turbulent fluid to distortion is elastic in character, with incremental Reynolds stress proportional to increment of total strain, and sufficient rigidity could stabilize the bounding surface. A simple flow model—an inviscid stream flowing over an elastic jelly—is examined and the condition for marginal stability is compared with the observed properties of the flow. The model leads to the conclusion that indentations of more than a critical wave-number are stable, and provides reasons for the comparatively simple form of the surface and for the occurrence of indentations in groups of about three. The relative values of entrainment constants in different flows of uniform density do not depend critically on the nature of the entrainment process provided that the main turbulent motion remains geometrically similar, but the correlation between entrainment constant and relative depth of the indentations found by Gartshore (1966) appears as a consequence of the 'elastic' control of the growth–decay cycle. Lastly, the properties of the engulfment mechanism are used to show that the entrainment constant for a jet is proportional to the square root of the ratio of ambient density to the average density inside the jet. In contrast, the corresponding result for engulfment controlled by an eddy viscosity is variation as the ratio of the mean of the ambient and inside density to the inside density. Observations of high-speed jets of water in air and air in water give some support to the 'elastic' hypothesis.

1. Introduction

A curious and characteristic feature of free turbulent flows is that, at any moment, there exists a well-defined surface separating the fluid in turbulent

motion from the surrounding fluid in the free stream, which is in irrotational motion. On one side, the vorticity is everywhere very small, while vorticity in the turbulent fluid is irregularly distributed and generally large. The surface is deeply indented and its presence was invoked in the first place to explain the observed intermittency of the output from a hot-wire anemometer placed near the mean position of the surface. Although twenty years have passed since the first observations of intermittency by Corrsin (1943), understanding of the phenomenon and of the part the surface indentations play in the entrainment of ambient fluid is still very incomplete. The difficulties of formulating theoretical models that will provide an adequate account of the observations do not diminish the importance of the phenomenon and there are a considerable number of experimental studies which have made clear the form and motion of the bounding surface. My intention is to set out the implications of the observations and then to develop a theoretical model that is capable of accounting for the surface behaviour, in particular the flow instability that leads to the characteristic growth–decay cycle of the indentations.

The observations under review are considered in four groups: (i) those using an 'intermittency' signal which indicates whether an anemometer is in turbulent or in ambient fluid, (ii) those using tracers that are carried and diffused only by turbulent fluid, (iii) those concerned with the irrotational motion in the ambient fluid, and (iv) experimental studies of the effects on the flow of artificial disturbances. Although many of the observations refer to other flows, their discussion will be in terms of two-dimensional wake flow behind a cylinder for reasons of verbal convenience. The notation follows the usual pattern: Ox is in the direction of the free stream and Oz along the axis of the cylinder, the components of the mean velocity are (U, V, O) and of the turbulent velocity fluctuation (u, v, w).

2. Measurements with an intermittency signal

Essentially, an 'intermittency' signal always has one of two values depending on whether the sensing head is at that moment within turbulent or non-turbulent fluid. In practice, the signal is emitted by a discriminator circuit which responds only if the magnitude of the output from an appropriate hot-wire assembly has exceeded a threshold value within a short time interval, the 'memory' time. The most suitable assembly is one responding to a component of the fluid vorticity as used by Corrsin & Kistler (1954), but, although vorticity is the real distinction between the two regions, simple gradients of the velocity fluctuation can be obtained from less complex wire assemblies and are equally suitable at high Reynolds numbers of flow. The magnitude of the threshold value needs only to be set above the natural fluctuation level in the ambient fluid, but the choice of the memory time raises problems. It must be long enough to bridge the time gaps while the anemometer signal passes through zero and its magnitude is less than the threshold value, but short enough to ensure that the intermittency signal becomes zero promptly when the anemometer passes into undisturbed fluid. The difficulty of choosing a memory time reflects the difficulty of defining the exact position of the bounding surface and becomes progressively

less as the Reynolds number of the flow increases and the size of the smallest eddies decreases. The surface position cannot be defined more closely than the length scale of the smallest eddies contributing to the vorticity fluctuations, which is comparable with the Kolmogoroff length scale, $l_s = \nu^{\frac{3}{4}}\epsilon^{-\frac{1}{4}}$ (ν is the kinematic viscosity, ϵ is the rate of dissipation of turbulent energy by viscous forces). It follows that the optimum memory time is of order l_s/U_c, where U_c is the convection velocity of the smallest eddies. For a particular flow, the memory time varies nearly as the $-\frac{3}{4}$-power of the Reynolds number.

Supposing these practical problems to be solved, we have at our disposal a signal proportional to a function $\delta(\mathbf{r}, t)$ which is one or zero as the point $\mathbf{r}$ is at time t within turbulent or within undisturbed fluid. The simplest measurement is of its mean value, which gives the proportion of time that the sensor is within turbulent fluid, and which is known as the intermittency factor. The distribution of $\overline{\delta}$ has been studied for a variety of flows (plane wake Townsend 1949, axisymmetric jets Corrsin & Kistler 1954 and Gartshore 1966, plane jet Bradbury 1965, boundary layers Corrsin & Kistler 1954, Klebanoff 1954), and it is broadly similar in all. Near the central plane of the flow (on the axis for axisymmetric flows or near the wall for boundary layers), the intermittency factor is one and it begins to decrease sharply about half-way to the extreme limit of mean velocity variation (figure 1). At the extreme limit it is still appreciable.

If the surface displacement is always a single-valued function of position in the axial plane, i.e. if it is simple and not folded over on itself, the variation of $\overline{\delta}$ with distance from the central plane is a reproduction of the integrated probability distribution function for the displacement. The distribution function so determined is nearly normal, which has led Corrsin & Kistler to conclude that the surface displacements arise from a process of generalized turbulent diffusion. A comparison of the distributions for various distances from the flow origin shows that, on the average, the surface advances into the undisturbed fluid at a rate comparable with but rather less than the root-mean-square turbulent velocity.

The intermittency signal may be analysed in much the same way as the turbulent velocity fluctuation, and Corrsin & Kistler (1954) have measured a variety of statistical parameters for the signal obtained from a boundary layer in zero pressure gradient. In the present context, the most interesting of their results are the distributions of the time intervals between changes in the signal. In the outer part of a boundary layer, it is permissible to use the Taylor approximation that the flow pattern, including the bounding surface, is swept past the sensor at the local mean velocity without undergoing appreciable change. Then a time interval τ in the record is equivalent to a space interval of $U_c\tau$ in the direction of flow, where U_c is the convection velocity or, very nearly here, the mean velocity. Their results for the mean values of l_1, the interval in turbulent fluid, and of l_2, the interval in irrotational fluid, are expressed conveniently in terms of η_0, the distance from the wall at which $\overline{\delta} = \frac{1}{2}$. Bradbury (1965) has measured the mean frequency with which δ changes from 0 to 1 in a plane jet, and, on the assumption that the effective convection velocity is the mean velocity in the jet, the corresponding values of $\bar{l}_1 + \bar{l}_2$ are included in table 1. It is evident

that the mean intervals are rather larger than the mean distance of the bounding surface from the 'centre' of the flow and considerably larger than the standard deviation of the surface displacement from its mean position, $y = \eta_0$. Corrsin

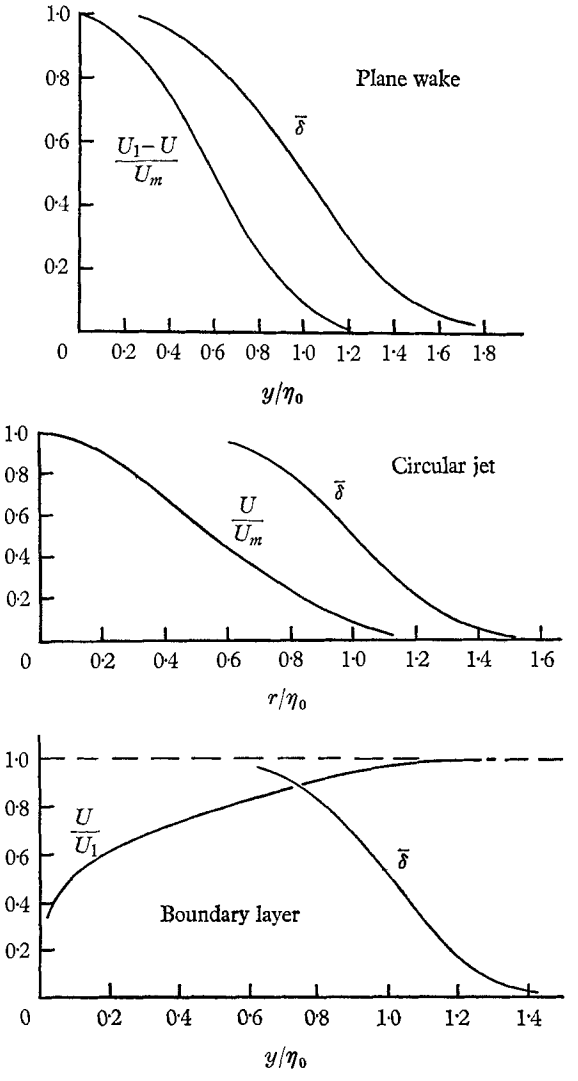

FIGURE 1. Distributions of mean velocity and intermittency factor for a wake, a circular jet and a boundary layer.

& Kistler (1954) have pointed out that $(\bar{l}_1 + \bar{l}_2)^{-1}$ is the average number per unit length of intersections of the surface by a line through the sensor and parallel to Ox, and that, if the surface displacement $\eta - \eta_0$ and its gradient $\partial\eta/\partial x$ are statistically independent and normally distributed,

$$(\bar{l}_1 + \bar{l}_2)^{-1} = \frac{1}{2\pi}\left[\overline{\left(\frac{\partial\eta}{\partial x}\right)^2} \Big/ \overline{(\eta - \eta_0)^2}\right]^{\frac{1}{2}} \exp -\frac{1}{2}\left(\frac{y - \eta_0}{\sigma}\right)^2. \tag{2.1}$$

The values of $\overline{(\partial\eta/\partial x)^2}$ have been calculated on this assumption.

An interesting point about the observations is that the length scale

$$[\overline{(\eta-\eta_0)^2}/\overline{(\partial\eta/\partial x)^2}]^{\frac{1}{2}},$$

which is analogous to the Taylor micro-scale, λ, is about one-third of the half-width of the flow, although the Reynolds numbers are large. If $\phi(k)$ is the power spectrum of $\eta-\eta_0$, $k^2\phi(k)$ is the power spectrum of $\partial\eta/\partial x$ and the length scale is the reciprocal of the 'radius of gyration' of the spectrum about the vertical axis.

Flow	$\bar{\delta}$	l_1/η_0	l_2/η_0	$(l_1+l_2)/\eta_0$	σ/η_0	$[\overline{(\partial\eta/\partial x)^2}]^{\frac{1}{2}}$
Boundary layer	0·75	2·2	0·85	3·0		
(Corrsin &	0·50	1·6	1·2	2·8	0·17	0·38
Kistler)	0·25	1·05	2·0	3·0		
Plane jet	0·75	—	—	2·3		
(Bradbury)	0·50	—	—	2·0	0·22	0·69
	0·25	—	—	2·3		

N.B. The deviation of the ratios l_1/l_2 from the correct value of $\bar{\delta}/(1-\bar{\delta})$ is due to sampling errors consequent on the use of comparatively short lengths of oscillograph record.

TABLE 1

In figure 2, possible relations between two spectra are sketched and compared with the relations for the spectra of a turbulent velocity fluctuation and its space derivative. Consideration of the possibilities shows that, if the slope spectrum is dominated by large wave-numbers, the surface displacement depends on very small wave-numbers much less than $2\eta_0^{-1}$. It seems certain that the displacement spectrum is large for wave-numbers around $2\eta_0^{-1}$, and that larger wave-numbers contribute neither to the displacement nor to the slope, if we regard folding on the scale of the Kolmogoroff length as being beyond the limit of resolution.

The statistical distributions of l_1 and l_2 are broadly similar in form after allowance is made for the different mean values when $\bar{\delta}$ is not equal to one-half. The significance of this is that for most of the time the surface is statistically symmetrical about its mean position.

The intermittency signal may be combined with other signals to measure mean values of flow parameters within the turbulent fluid. For our purposes, the most interesting of these is the mean flow velocity within the turbulent fluid, obtainable from the ordinary mean velocity and the mean product, $\overline{\delta u}$. Measurements in a turbulent wake at a cylinder Reynolds number of 8200 show that the difference in mean velocity within and without the turbulent fluid is no more than 5% of the maximum velocity difference in the flow (Townsend 1956). It is not difficult to show that the difference cannot exceed the root-mean-square velocity fluctuation in the stream direction, about 25% of the maximum velocity difference, but the actual figure is substantially less.

To summarize the conclusions from studies of the intermittency signal,

(i) the bounding surface is well defined for large Reynolds numbers of flow, with a mean position about three-quarters of the way from the flow centre to the limit of mean velocity variation,

(ii) the scales of the surface indentations are comparable with the total width of the flow and there is little folding on the smaller scales which cover the range of eddy sizes in the turbulent flow,

(iii) the depths of the indentations are normally distributed to a fair approximation, and

(iv) the average velocity difference between the turbulent and non-turbulent flow is small but not negligible, perhaps 5 % of the maximum velocity difference.

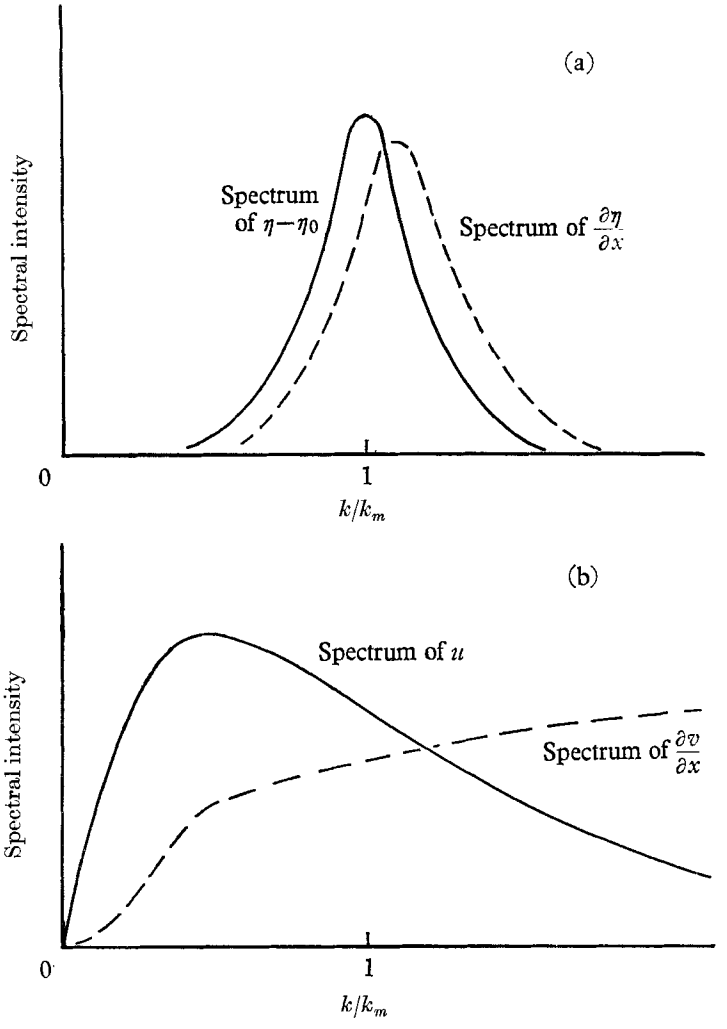

FIGURE 2. Relative dispositions of the power spectra for a random variable and for its derivative: (*a*) with a narrow-band spectrum as proposed for $\eta-\eta_0$; (*b*) with a wide-range spectrum of the kind characteristic of turbulent velocity fluctuations.

3. Visualization techniques

The turbulent fluid may be made visible and distinguished from the ambient fluid by introducing scalar contaminants into it. One is heat, simply introduced by heating the wake-producing cylinder or the jet and easily observed by use

of schlieren or shadow-graph techniques. Alternatively, smoke may be introduced into air flows or coloured dye into liquid flows. All these contaminants remain in the turbulent fluid because the molecular diffusivity is invariably too small to allow appreciable spread into the irrotational flow. High-speed photographs of axisymmetric flows show clearly the bounding surface, confirming its sharp definition. When heat is used as the contaminant, it can be seen that the gradients of refractive index, which determine the light and shade pattern in a schlieren photograph, are distributed nearly uniformly within the surface (e.g. plate B 28 of *Turbulent flows and heat transfer*, Lin 1959).

The usefulness of visualization techniques lies in the possibility of studying development of flow structures, and ciné photographs of a turbulent wake show that the indentations grow and decay in a cyclic pattern when observed moving with the ambient fluid. After a quiescent period, groups of indentations appear and grow to large amplitudes. They then engulf ambient fluid with rapid spreading of the turbulent region, lose energy and disappear. After another quiescent period, another group of indentations arise, not related to the preceding group, but with a larger scale appropriate to the increased width of the flow, and the cycle is repeated. At times, the pattern of the indentations during growth bears a strong resemblance to the Kármán streets of eddies which form behind a cylinder at Reynolds numbers in the range 45–200, but they arise locally and are not related in frequency to the eddies shed by the cylinder (Grant 1958; Keffer 1965).

Visualization studies tend to confirm the conclusion from the analysis of intermittency signals that the indentations are produced for the most part by movements on scales comparable with the flow width. Figure 3 (plate 1) shows photographs of dye released into the turbulent wake behind a circular cylinder through a small hole in the cylinder. The Reynolds number of the flow (about 1200) is too small for a well-defined bounding surface, but the contrast in complexity of the dye boundaries when viewed parallel to the cylinder and at right angles to it is clear. In the first view, the dye remains within the bounding surface and its outline is determined by the form of the surface over a range of z comparable with the wake width. In the second view, the dye outline depends on the spread in the Oz-direction and the 'bounding surface' between coloured and transparent fluid is distorted by turbulent eddies that are indifferent to the surface. The fine details visible in the second view are a consequence of dye transport by all scales of the turbulent motion, while the simpler outlines of the first view indicate a simpler spectrum for motion at the bounding surface.

4. Irrotational motion of the ambient fluid

The surface separating turbulent, eddying fluid from ambient, irrotational fluid is not a material surface which moves with the fluid. It advances into the ambient fluid by a process of vorticity diffusion and subsequent amplification of the diffused vorticity by straining, but the process of small-scale 'nibbling' must be nearly uniform over the surface. If we seek to relate the irrotational motion of the ambient fluid to the movements of the surface, we should consider the potential flow caused by motion of a boundary across which there is a steady

suction. On the average, i.e. over the whole growth–decay cycle, the surface slopes are fairly small (table 1), and the irrotational motion is nearly that produced by the motion of an impermeable surface coinciding with the bounding surface added to a uniform velocity which is the difference of the mean rate of advance of the surface and the suction velocity. On this basis, Phillips (1955) showed how the irrotational fluctuations outside the turbulent flow are related to the normal velocities produced by the movement of the surface relative to the free stream. If the spectrum function of the normal velocities is of the most general form compatible with the condition of incompressibility, the mean square of the fluctuation velocity falls off as $(y-\eta_0)^{-4}$ for large values of y/η_0. Bradbury (1965) has shown that the 'turbulent' intensities in the ambient fluid do vary in this way with a value of η_0 close to the mean position of the surface.

If the irrotational fluctuations are caused by movements of the bounding surface, their spectrum depends on the instantaneous spectrum of the surface movements, and, if the surface movements have a well-defined convection velocity, the fluctuations will have the same convection velocity.† Since unambiguous measurements of the irrotational motion must be made at some distance from the surface, the convection velocity is that of the larger-scale indentations. Reports of observations related to the convection velocity are few and scattered. Near the mixing zone of a turbulent axisymmetric jet, Davies (1964) found the convection velocity to be nearly one-half of the core velocity, both in the potential core and outside the mixing zone. Bradshaw, Ferriss & Johnson (1964) have measured the frequency spectrum of the fluctuations and find that it has the same shape as the spectrum in the region of maximum shear, but with a scale factor indicating a convection velocity of $0{\cdot}65U_m$, where U_m is the excess of maximum velocity over the ambient velocity. By comparing the longitudinal correlation function with the frequency spectrum at a point, Franklin & Foxwell (1958*a*) find a convection velocity for the near-field pressure fluctuations of about $\frac{1}{2}U_m$. Wills (1964) finds that the convection velocity of the v fluctuations exceeds that of the u fluctuations near the edge of the flow, which, in view of the dominance of v fluctuations in the irrotational flow, points to a convection velocity substantially different from the velocity of the free stream. On the whole, it seems certain that the convection velocity of the irrotational fluctuations is intermediate between the central velocity and the stream velocity.

Even for a jet of nearly sonic velocity, the pressure fluctuations within one or two exit diameters are nearly those of the irrotational flow and, with a definite convection velocity considerably larger than the irrotational velocity fluctuation u_r, the pressure fluctuation is given by

$$p = -\rho U_c u_r. \tag{4.1}$$

Franklin & Foxwell (1958*b*) give measurements of the intensities of the pressure fluctuations near the mixing zone of a circular jet. One jet diameter from the outer

† Convection velocity is a term used to describe the quotient of spatial by time displacement for maximum space–time correlation. For an unchanging pattern it is the speed with which the pattern moves. It may be quite different from the fluid velocity.

edge of the mixing layer, their intensity contours show that

$$(\overline{p^2})^{\frac{1}{2}} = 1{\cdot}8 \times 10^{-3} \rho U_m^2,$$

and an extrapolation of their results to the presumed mean position of the bounding layer (using their lateral traverse) indicates that there

$$(\overline{p^2})^{\frac{1}{2}} \doteqdot 1{\cdot}5 \times 10^{-2} \rho U_m^2.$$

This value may be compared with

$$(\overline{p^2})^{\frac{1}{2}} = \rho U_c (\overline{u_r^2})^{\frac{1}{2}}, \tag{4.2}$$

obtained from (4.1), to give

$$(\overline{u_r^2})^{\frac{1}{2}}/U_m = 0{\cdot}03,$$

on the presumption that $U_c/U_m = \frac{1}{2}$. Bradshaw *et al.* (1964) have measured the turbulent intensities in a similar jet and find that $(\overline{v_r^2})^{\frac{1}{2}}/U_m \doteqdot 0{\cdot}08$ in this region. A considerable part of the measured intensity belongs to the rotational flow, and, in potential flow,

$$\overline{u_r^2} + \overline{w_r^2} = \overline{v_r^2}, \tag{4.3}$$

so that the observed pressure fluctuations are broadly consistent with the observed turbulent intensities and a convection velocity of magnitude comparable with $\frac{1}{2}U_m$.

5. Response to an external disturbance

The observations so far described were made in undisturbed flows and may not form the best guide to the mechanics of the flow. Better understanding may be found by study of disturbed flows in which certain elements of the mechanism are magnified or suppressed. Clauser (1956) has suggested that a turbulent boundary layer may be regarded as a 'black box' containing a control mechanism which regulates the intensity of the turbulence and the spread of the flow, and, like other control systems, useful information about the nature of the mechanism can be obtained by observing the response to external disturbances of suitable form. The difficulty of the method is to find a disturbance that produces a substantial effect on the flow, the only success to date being the effect on a turbulent wake of a suddenly imposed plane straining in the transverse direction, i.e. $\partial V/\partial y = -\partial W/\partial z < 0$. These measurements, by Reynolds (1962) and by Keffer (1965), are concerned with continuous straining and lead to fundamental changes in the flow, but the nature of the changes shows clearly the nature of the flow patterns that cause the surface indentations.

Both from correlation measurements and from observations of a dye-containing wake, Grant (1958) has concluded that the 'large eddies' that cause the indentations† resemble short trains of eddies arranged as in a Kármán street, differing from the prototype behind a circular cylinder by occurrence in groups of perhaps three eddies on each side, by impermanence and by restricted extent

† Grant reported also large 'inclined' eddies, but their circulation is in the (xOz)-plane and they cannot cause indentations.

in the direction parallel with the cylinder. Circulation in the eddy systems is nearly confined to the plane Oxy at right angles to the cylinder axis Oz, and imposition of a plane straining with extension along the Oz-axis is expected to increase the energy of the system and the velocities of circulation. Reynolds and Keffer find that the first effect is a greatly increased rate of spread of the wake, clearly caused by increased intensity of the motions responsible for the distortion of the bounding surface. Visualization studies show that the periodic indentations become far more striking and they do not disappear with further development but remain permanent features of the flow (Keffer 1965). It is clear that systems of eddies closely resembling those postulated by Grant exist in a normal wake and are the major agents for the distortion of the bounding surface and the spread of the turbulent fluid.

6. Mechanism of the large eddies—equilibrium hypothesis

Lateral spreading of a turbulent flow involves conversion of irrotational ambient fluid to turbulent fluid, a process that depends in detail on small-scale diffusion of vorticity across the bounding surface. However, the folding of the surface by the large eddies can increase greatly the rate of conversion, which is controlled by the intensity of the large eddies. The large eddies might arise from the general turbulent motion, but their degree of organization suggests that they derive energy from the organized mean flow, and that the remaining turbulent motion of smaller scales merely resists their growth by absorbing some of their energy. Then a sufficiently high intensity of the turbulent motion may prevent further growth of the large eddies or even destroy existing ones. Further, lateral spreading of a free turbulent flow is accompanied necessarily by transfer of energy from the mean flow to the turbulent motion, and the greater the rate of spread the greater the rate of energy transfer. So, if an unusually vigorous set of large eddies appeared in the flow, they would cause a large increase in the rate of production of turbulent energy which, in time, might lead to turbulent intensities sufficient to destroy them. The equilibrium hypothesis assumes that the large eddies are the principal agents of the entrainment process and that their average intensity is set by the operation of a control cycle whose elements are: growth of large eddies → rapid entrainment → increase of turbulent intensity → additional damping of the large eddies → decrease in intensity of large eddies.

A feedback control system of this kind may or may not be stable; that is, the level of the controlled quantity may remain nearly steady, or it may oscillate with considerable amplitude around the value for unstable equilibrium. Only for the rather special flow in a distorted wake does the intensity of the large eddies remain steady and the more usual behaviour is the oscillation of the growth–decay cycle described by Grant. The observed instability derives from two characteristics of the system. First, the spreading of the flow means that any group of large eddies becomes progressively smaller compared with the flow width and so less able to extract energy from the mean flow. Secondly, the delay in response of the elements of the control cycle allows overshooting of the

equilibrium intensity and is favourable to oscillation. Observations of the growth–decay cycle are consistent with the following scheme:

(i) During a period of quiescence, the turbulent intensity is too large to permit growth of large eddies, but, in their absence, entrainment is weak and the intensity decreases until the flow is unstable to development of large eddies of suitable scale.

(ii) Once the flow is unstable, suitable components of the existing turbulence grow and develop into a large eddy system which causes rapid entrainment.

(iii) The rapid entrainment leads to an increase of turbulent intensity, making the flow once more stable to growth of large eddies, and the existing eddies lose energy to the main turbulent motion, and another period of quiescence begins.

(iv) The cycle recurs but the flow width is considerably larger and the next set of large eddies are also larger. If the equilibrium hypothesis is accepted, the average level of the turbulence is near the value for neutral stability of the flow to eddy disturbances that can develop into a system of big eddies.

The first attempt to apply the hypothesis to predict the rate of spread of a turbulent flow assumed that the action of the main turbulent motion on the large eddies can be represented by a coefficient of eddy viscosity equal to the value describing the rate of spread of the mean flow (Townsend 1951). The stability problem was further simplified by ignoring the existence of the bounding surface and assuming the eddy viscosity to act everywhere and not just inside the boundary. In this form, the model leads to a surprisingly accurate value for the effective eddy viscosity in a plane wake (Townsend 1951, 1956) and explains satisfactorily the different values of the flow constants ('Reynolds numbers' formed from flow width, variation of mean velocity and *eddy* viscosity) in jets, wall jets and wakes (Gartshore 1966). As a description of the mechanics of generation of the large eddies, the model is much less satisfying. The basic difficulty is that the pressure field on the bounding surface caused by its motion relative to the inviscid ambient fluid cannot be balanced by viscous-type stresses proportional to rates of strain and all disturbances are unstable. For example, in a flow with a constant velocity V of the turbulent fluid relative to the free stream, disturbances of wave-number k grow as $\exp(\frac{1}{2}kVt)$ if $V/(k\nu)$ is large, and as $\exp(\frac{1}{2}V^2t/\nu)$ if $V/(k\nu)$ is small (see appendix). Observations of dyed wakes suggest strongly that the growth of large eddies sets in suddenly and so that a critical condition for growth exists. The presence of a gradient of mean velocity in the turbulent fluid is not likely to change the pattern of essentially Kelvin–Helmholtz instability.

An explanation of the sudden appearance of large eddies after a quiescent period was given by Grant (1958) in terms of stress-releasing behaviour, in which Reynolds stresses stored in the fluid are re-aligned by the large eddies so that they can release their energy. An essential feature is a non-Newtonian behaviour of the turbulent fluid with persistence of stresses after an element of fluid passes into a different environment. That the Reynolds stresses produced by distortion of turbulent fluid have a qualitative resemblance to those in a visco-elastic liquid is confirmed both by measurements of grid turbulence in a distorting duct (Townsend 1954), and by the theory of the behaviour of isotropic turbulence

undergoing very rapid distortion (figure 4). The initial response of the turbulent fluid is to develop additional Reynolds stresses nearly proportional to the total strain, and a uniform rate of strain produces stresses which increase until the total strain ratio is of order three. It seems likely that the response of the turbulent fluid to the initial growth of the indentations is closer to that of an elastic solid than that of a viscous fluid and that the pressure field on the surface is balanced by 'elastic' stresses for neutrally stable disturbances.

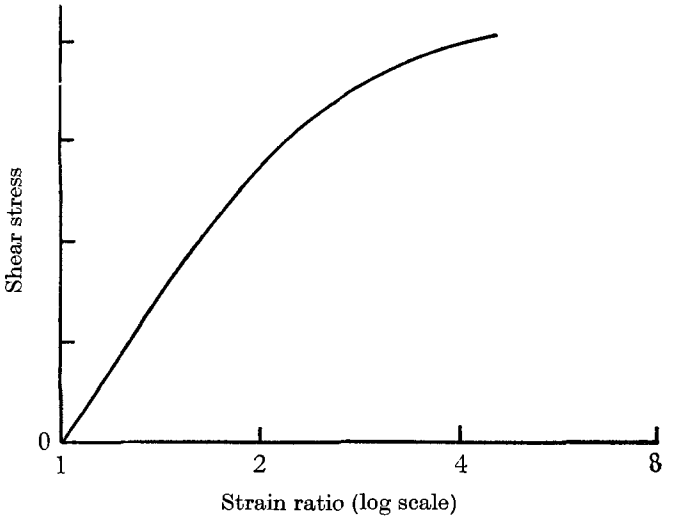

FIGURE 4. Stress–strain diagrams for turbulent fluid (based on results from Townsend 1954).

The 'elastic solid' is unusual in that it contains a basic distribution of mean velocity acted on by Reynolds stresses which are nearly homogeneous in the flow direction, and only the incremental stresses caused by the developing indentations are related to the incremental strains by an elastic equation. The elastic behaviour depends on the nature of the main turbulent motion, which is strongly anisotropic. In spite of this, let us assume that the stress–strain relationship is that of an incompressible solid of rigidity n; i.e. the incremental stresses are

$$p_{ij} = n\left(\frac{\partial \xi_i}{\partial x_j} + \frac{\partial \xi_j}{\partial x_i}\right) - \delta_{ij} p, \tag{6.1}$$

where ξ_i is the incremental displacement of a fluid particle, and p is the hydrostatic pressure. With this assumption, it would be possible to investigate the stability of a flow consisting of turbulent 'elastic' fluid initially between the planes $y = \pm h$, with a specified basic distribution of mean velocity and bounded by inviscid fluid at rest. The calculations would be tedious and it seems clear that the basic features of the instability are similar to those of the Kelvin–Helmholtz vortex sheet so that it can be examined with a much simpler model. We suppose that all of the turbulent fluid involved in the disturbance is moving with the same velocity V relative to the free stream, and then it is not

difficult to show that (see appendix) antisymmetric disturbances of wave-number k in the direction of flow propagate with phase velocity c given by

$$c^2(c-V)^2 = n^2[4(1-c^2/n)^{\frac{1}{2}}\tanh\{kh(1-c^2/n)^{\frac{1}{2}}\}-(2-c^2/n)^2\tanh kh]. \quad (6.2)$$

For large kh and V less than $1{\cdot}79n^{\frac{1}{2}}$, there are two real roots and the system is stable to small disturbances, but, with slightly larger values of V, waves with phase velocities relative to the jelly of approximately $0{\cdot}63n^{\frac{1}{2}}$ grow exponentially in amplitude. For small values of kh, waves grow exponentially with phase velocity equal to V and with amplitude varying as $\exp(kh)^{\frac{1}{2}}kVt$.

To use these results, the effective rigidity of the turbulent fluid is needed. In the initial stages of distortion of isotropic turbulence, the rapid distortion theory (see equation (4.3.3), Townsend 1956) leads to

$$n = \tfrac{2}{5}\overline{u^2}, \quad (6.3)$$

but it is probable that additional distortion of the fully strained turbulence is opposed by a larger rigidity, possibly as large as $\frac{1}{3}\overline{q^2}$. For a wake, which satisfies the condition of parallel flow better than jets, $(\overline{u^2})^{\frac{1}{2}} = 0{\cdot}3U_m$, where U_m is the maximum velocity defect, and so the convection velocity relative to the irrotational fluid of the neutrally stable disturbances of large kh would be $0{\cdot}22U_m$ or $0{\cdot}35U_m$, depending on which estimate of the rigidity is adopted. Both values are less than the observed convection velocity of about $0{\cdot}5U_m$, a discrepancy that may arise from the crudeness of the model, but which is more likely to be caused by use of the mean value of the turbulent intensity rather than the value when the flow is neutrally stable. In the growth–decay cycle, neutral stability occurs during the quiescent phase when the turbulent intensity is larger than the average over the cycle. Allowing for this difference, the observations are consistent with the suggestion that the large eddies arise from an instability controlled by elastic behaviour of the turbulent fluid.

7. The shape of the bounding surface

Consideration of the simplified flow model has shown that the turbulent intensity in a wake has nearly the magnitude necessary to stabilize the flow against development of moderately large eddies during the quiescent period of the growth–decay cycle. Two assumptions are made: (i) the eddies are so large that the main turbulent motion is smaller in scale and the rigidity is proportional to their turbulent intensity, and (ii) the real distribution of velocity in the turbulent fluid can be replaced by a step distribution with constant velocity equal to some effective velocity. If we consider the stability of the surface to smaller-scale displacements, both assumptions need modification. First, turbulent eddies of size larger than the scale of the disturbance respond to an average of the deformation over their extent and can contribute little to the elastic stresses that resist the deformation. Approximately, the effective rigidity for a disturbance of wave-number k depends on the turbulent intensity of eddy components of larger wave-numbers, say

$$n(k) = a\int_{bk}^{\infty} E(k')\,dk', \quad (7.1)$$

where a and b are constants of order unity, and $E(k)$ is the power spectrum of turbulent intensity. Secondly, the disturbance produced by a corrugation of wave-number k is confined within a depth of order k^{-1}, and, if the step distribution of velocity is to be used, the effective velocity V must be an average of the mean velocity in the disturbed layer and approximated by

$$V(k) = U(\eta_0 - c_1 k^{-1}), \tag{7.2}$$

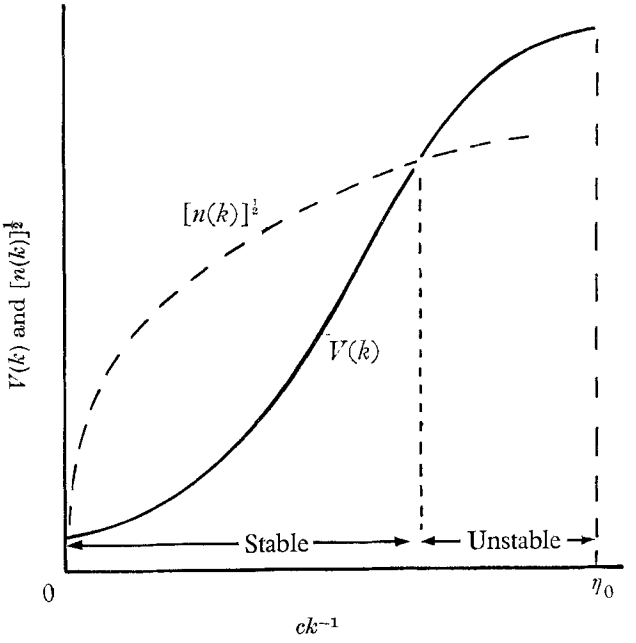

FIGURE 5. Stability diagram displaying relative values of effective velocity and rigidity over the range of wave-numbers, calculated from (7.2) and (7.1).

the mean velocity at a depth $c_1 k^{-1}$ within the turbulent fluid (where c_1 is another constant of order unity). Using results quoted above, indentations of wave-number k are unstable if $V(k)$ is greater than $1{\cdot}79[n(k)]^{\frac{1}{2}}$. If the wave-number lies within the inertial subrange of the spectrum, we have, from the Kolmogoroff theory of local similarity,

$$E(k) = C\epsilon^{\frac{2}{3}}k^{-\frac{5}{3}},$$

and the condition for instability is then that

$$V(k) > (\tfrac{3}{2}aC)^{\frac{1}{2}}(\epsilon b)^{\frac{1}{3}}k^{-\frac{1}{3}}. \tag{7.3}$$

Taking into account the fact that indentations of wave-numbers around η_0^{-1} are roughly in a condition of neutral stability, the stability condition (7.3) can be expressed in graphical form (figure 5). Notice that the intermediate range of eddy sizes is stable and that only the large eddies and, possibly, the smallest eddies can be unstable. The stability of the intermediate range of surface deformations explains the comparatively simple form of the surface and its sharpness.

The characteristic appearance of large eddies in groups of about three on each side of the flow is a natural consequence of the stability of small-scale

indentations and the variation of growth rate with wave-number. The origin of a group is a chance distortion of the bounding surface by essentially unorganized eddies of the turbulent motion and, if the group is to grow to large amplitude in the limited time available for growth, the form of the distortion must be characteristic of the energy-containing eddies of the turbulent motion. A possible disturbance is

$$\eta - \eta_0 \propto (x\cos\phi + z\sin\phi)\exp\{-\tfrac{1}{2}k_1^2(x^2+z^2)\}, \tag{7.4}$$

where k_1 is a wave-number characteristic of the turbulent motion and ϕ is the inclination to the Ox-axis of the 'wave-normal' of the single-wave group described by (7.4). If $k_1 h$ is small, both bounding surfaces are likely to be distorted antisymmetrically by a single chance grouping of the turbulent eddies, but distortions of the two surfaces should be independent if $k_1 h$ is large. In terms of Fourier components,

$$\eta - \eta_0 \propto \iint k\cos(\theta-\phi)\exp(-\tfrac{1}{2}k^2/k_1^2)\exp\{i(lx+nz)\}\,dl\,dn, \tag{7.5}$$

where l, n are wave-number components, $k^2 = l^2+n^2$, and $\theta = \tan^{-1} n/l$ is the inclination of the wave-number vector to the direction of flow. The original distortion is likely to contain comparable amounts of symmetric and antisymmetric components, and the two groups of components grow at different rates. The stability condition for symmetric disturbances is obtained from equation (6.2) if hyperbolic cotangents are substituted for the hyperbolic tangents, and it is clear that large wave-numbers are stable and that the growth rates of symmetric and antisymmetric disturbances become equal for large values of kh. In any event, the process of amplification increases the antisymmetry of the indentation although the effect is small for large wave-numbers.

To the linear approximation, each antisymmetric Fourier component grows exponentially with a logarithmic rate of $(kh)^{\frac{1}{2}}kV\cos\theta$ for small values of kh. For larger values of kh, growth occurs if $V(k)\cos\theta$ exceeds $1{\cdot}79[n(k)]^{\frac{1}{2}}$ and, over the whole range of kh, the logarithmic growth-rate may be approximated by the function

$$(kh)^{\frac{1}{2}}k(1-k/k_0)\,V\cos\theta, \tag{7.6}$$

where k_0 is the upper limit to the range of unstable wave-numbers. The growth rates for symmetric components are less, particularly for smaller wave-numbers. The interesting point is that the growth rate has a maximum value at $k = \frac{3}{5}k_0$ and so, after considerable amplification, Fourier components with wave-numbers near $\frac{3}{5}k_0$ dominate the disturbance. Near the maximum, the growth rate (7.6) may be approximated by

$$(kh)^{\frac{1}{2}}k(1-k/k_0)\,Vt = \alpha - \tfrac{1}{2}L_0^2(k-\tfrac{3}{5}k_0)^2, \tag{7.7}$$

where $\alpha = (\frac{3}{5})^{\frac{1}{2}}\frac{6}{25}k_0^{\frac{3}{2}}h^{\frac{1}{2}}Vt$, and $L_0^2 = \frac{175}{18}\alpha k_0^{-2}$. Neglecting differences of phase velocities between the components and replacing the Fourier amplitudes of the disturbance (7.4), $k\cos(\theta-\phi)\exp(-\frac{1}{2}k^2/k_1^2)$, by the value at maximum amplification, $k = \frac{3}{5}k_0$, $n = 0$, the shape of the amplified indentation is given by

$$\eta - \eta_0 \propto e^{\alpha}\cos\phi\exp[-\tfrac{1}{2}(x^2/L_0^2 + \tfrac{9}{25}k^2z^2\alpha^{-1})]\sin(\tfrac{3}{5}k_0x). \tag{7.8}$$

The result of the amplification is to produce a distortion of the bounding surface with the form of a wave group having crests in the Oz-direction and appreciable amplitude over a distance of about $5L_0$ in the Ox-direction and about $\frac{25}{3}\alpha^{\frac{1}{2}}k_0^{-1}$ in the Oz-direction. Since the wave-number of the group is $\frac{3}{5}k_0$, the number of crests visible is about $(3/2\pi)\,k_0L_0 = \pi^{-1}(175\alpha/18)^{\frac{1}{2}}$. Figure 6 shows the form of a group for $\alpha = 2{\cdot}5$, corresponding to a maximum growth ratio of 12.

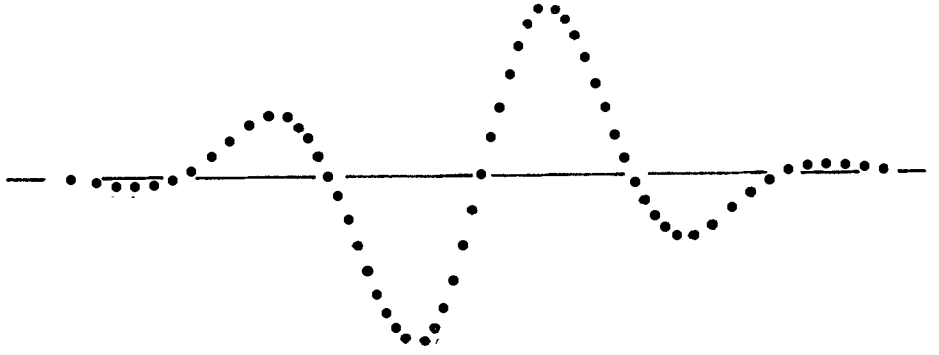

FIGURE 6. Shape of amplified wave group, calculated from (7.8) with $\alpha = 2{\cdot}5$.

The description may be compared with the large eddies in turbulent wakes photographed by Grant (1958) and by Keffer (1965). In a cylinder wake,

$$h = \eta_0 = 0{\cdot}4(xd)^{\frac{1}{2}} \quad \text{(Townsend 1956)},$$

the time available for growth is of order

$$\left[\frac{1}{h}\frac{dh}{d(x/U_1)}\right]^{-1},$$

i.e. $2x/U_1$ (U_1 is the stream velocity, d is the cylinder diameter), and the average wave-number of the large-eddy systems is about $2h^{-1}$† so that $k_0h = 3{\cdot}3$. Putting the convection velocity equal to the mean of the free-stream and axial velocities, $V = 0{\cdot}5U_1(d/x)^{\frac{1}{2}}$. Substituting these values in (7.7), $\alpha = 2{\cdot}5$ and the number of crests in a group is 2·3. The amplification ratio, about 12:1, is plausible and the number of crests close to that observed.

Antisymmetry of the indentations can arise from the process of amplification only if the most unstable wave-number is less than h^{-1} or by antisymmetry of the initial disturbance. The numerical values for the turbulent wake show that any antisymmetry must derive from the initial disturbance, and this is unlikely in view of the small scale of the turbulent motion. One would expect to find groups of about three crests on both sides of the wake without appreciable correlation between groups on opposite sides. Keffer concludes from a study of his photographs that there is no correlation but Grant came to the opposite

† Photographs by Keffer, taken just inside the distorting channel, show wave-numbers of about $3h^{-1}$, but these large eddies have been amplified and are characteristic of the wake before it entered the distortion and underwent an abnormally rapid expansion. In a normal wake, the relative wave-number must be rather less. Photographs by Grant are less clear but indicate an average wave-number near $2h^{-1}$.

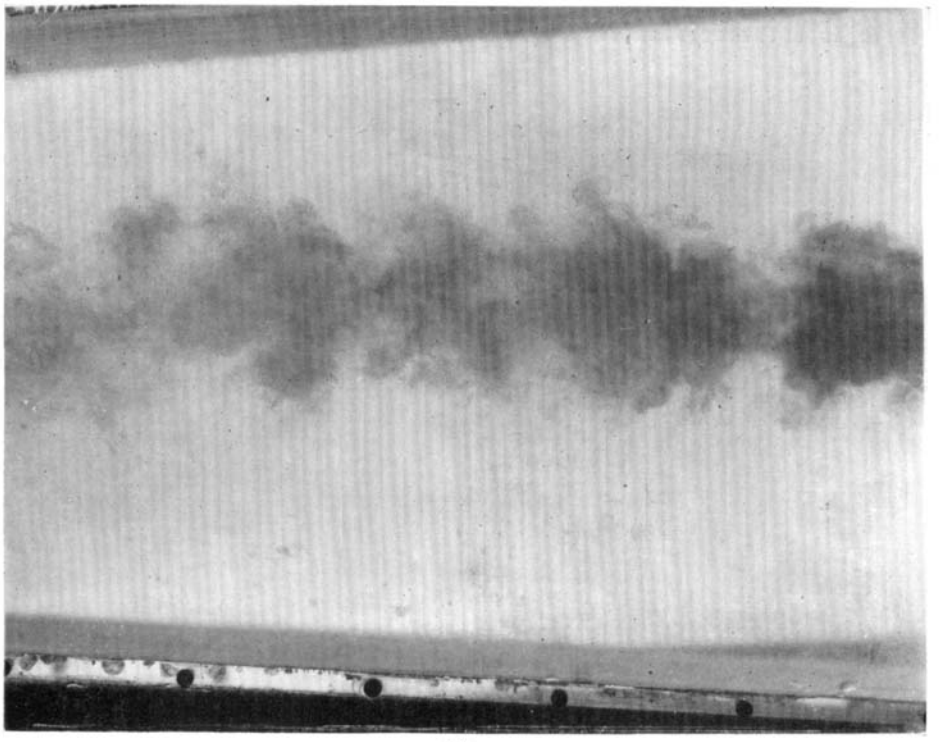

(*a*)

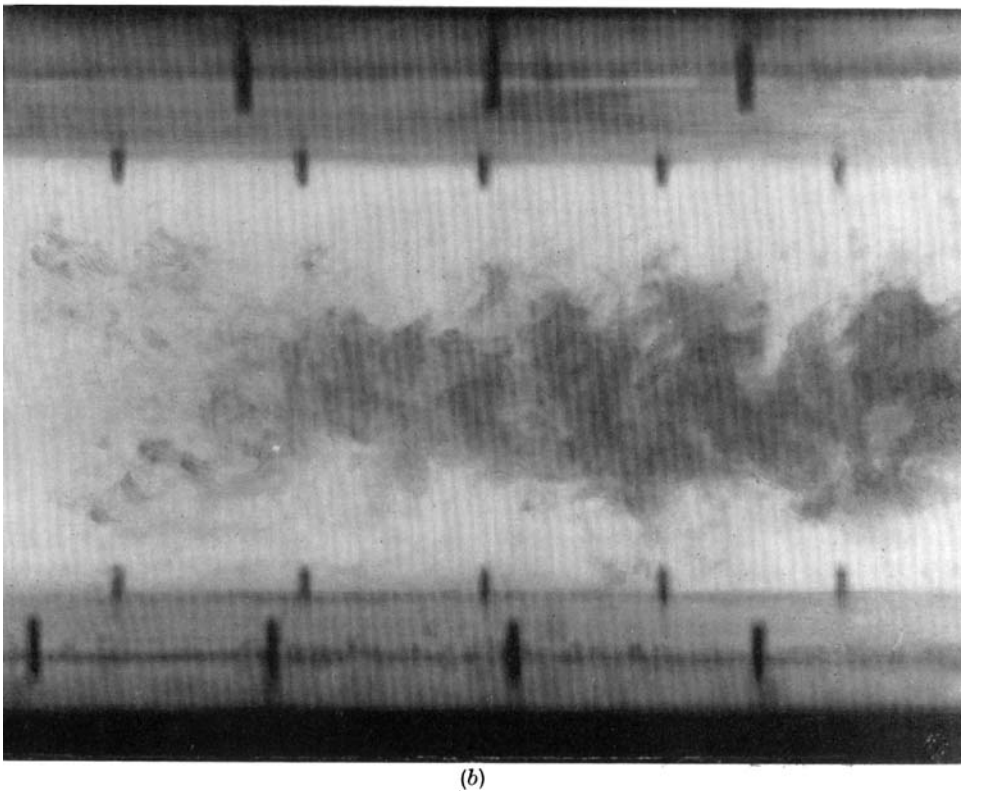

(*b*)

FIGURE 3. Photographs of the wake of a towed cylinder, made visible by the discharge of dye through a small hole at the rear of the cylinder; (*a*) seen along a line parallel with the cylinder axis; (*b*) seen along a line normal to the plane of the wake. (The width of the channel is about 12 cm, the cylinder diameter 3 mm, and the Reynolds number about 1200.)

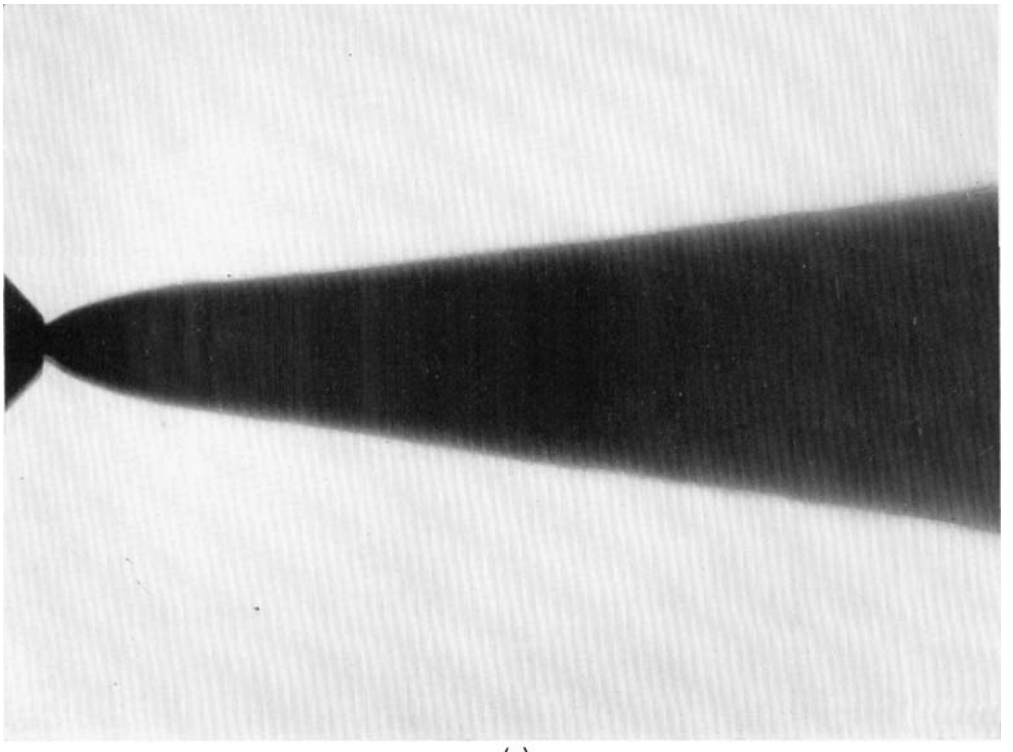

(*a*)

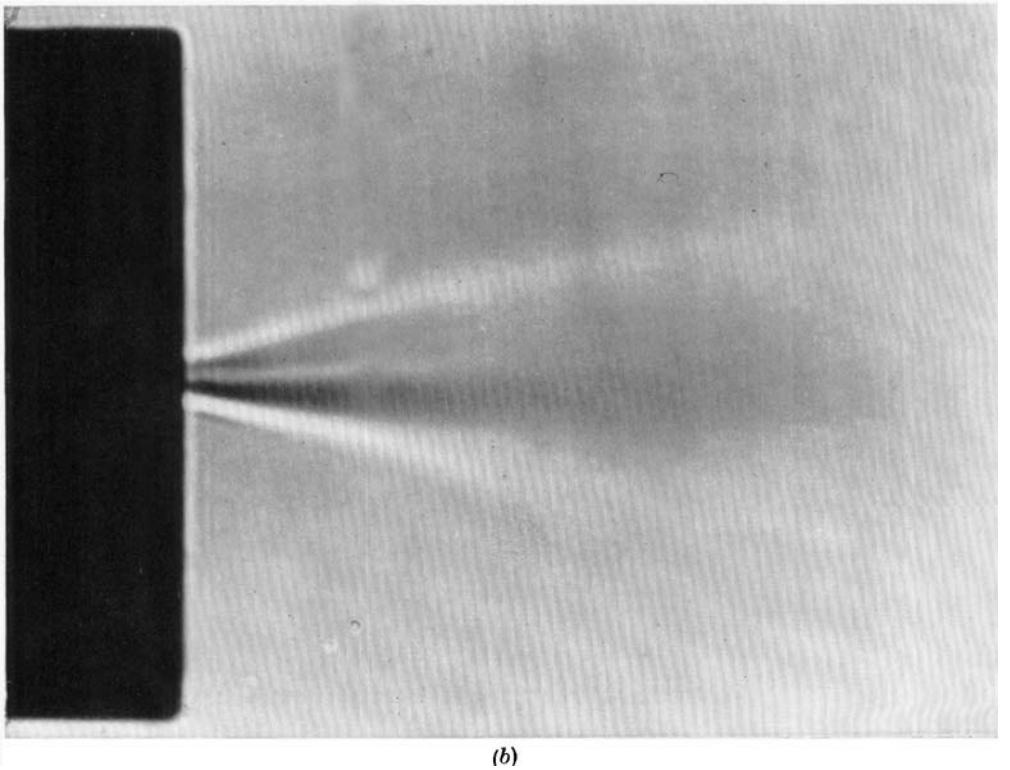

(*b*)

FIGURE 8. For legend see facing page.

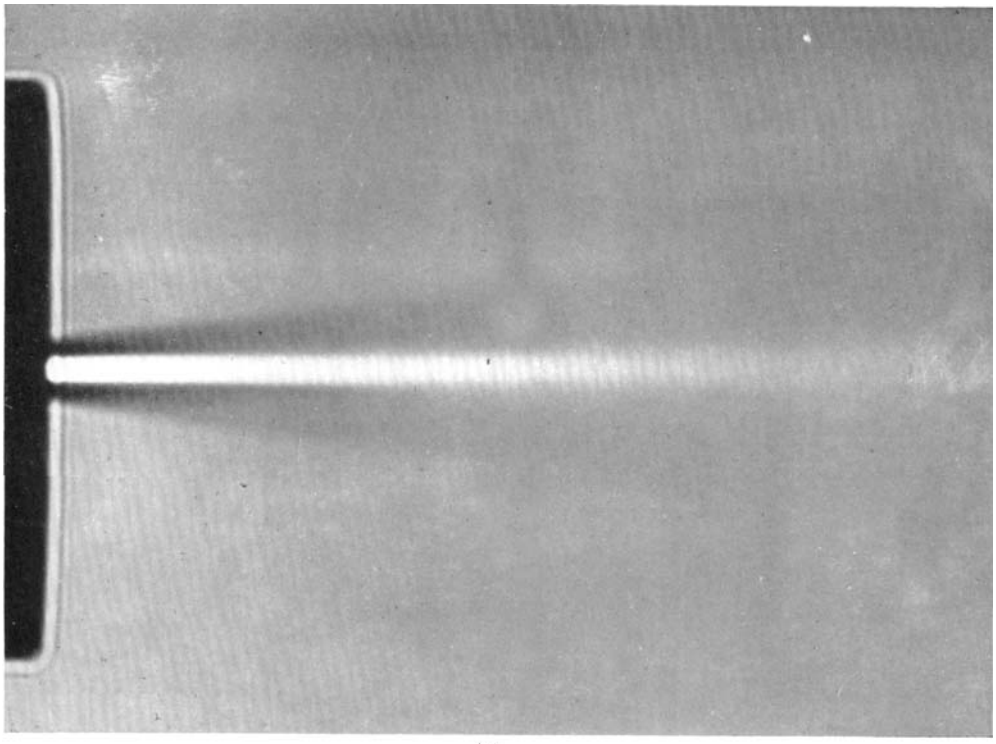

(*c*)

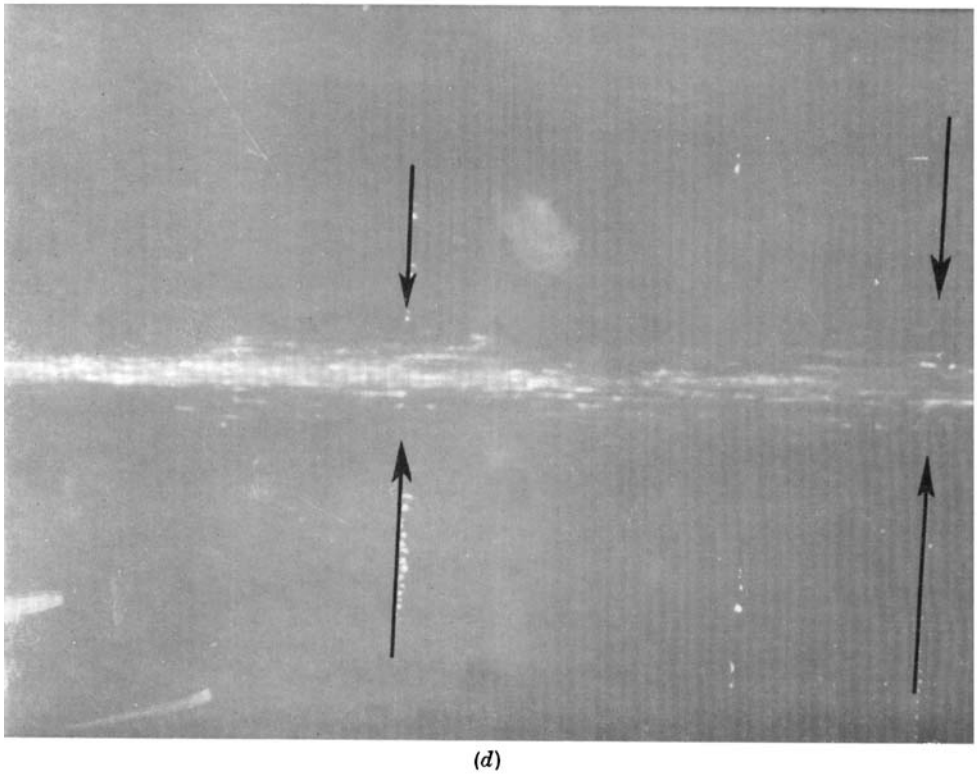

(*d*)

FIGURE 8. Photographs of inhomogeneous jets with various ratios of density of discharged fluid to density of ambient fluid: (*a*) air into water, ratio = 0·0015; (*b*) hydrogen into air, ratio = 0·07; (*c*) carbon dioxide into air, ratio = 1·5; (*d*) water into air, ratio = 650. (On (*d*), the two marked lines are 10 cm apart, and the jet orifice was about 40 cm to the left of the first marker.)

conclusion. In jets, the characteristic values of kh are even larger and it seems certain that the groups of large eddies arise independently on the two sides of the flow.

8. Variations of entrainment constant

In a self-preserving flow, the bounding surface advances into the ambient fluid at an average velocity that is a constant proportion of the local velocity scale of the flow, but one that is different in different kinds of flow. The ratio

Quantity	Wake	Jet	Boundary layer
β	0·40	0·18	0·048
σ/η_0	0·38	0·22	0·17
$(\overline{q^2}/U_m^2)_{y=0}$	0·21	0·13	0·08
$(\overline{q^2}/U_m^2)_{\max}$	0·24	0·15	0·08
$\lvert\overline{uv}\rvert_{\max}/U_m^2$	0·061	0·025	0·0105
L_u/η_0	0·5	0·55	0·7
η_0/l_0	2·1	2·0	2·15
$\left[\overline{\left(\frac{\partial\eta}{\partial x}\right)^2}\Big/\overline{(\eta-\eta_0)^2}\right]^{\frac{1}{2}}\eta_0$	2	3·1	2·6
Lateral rate of strain $y=0$	0	0·09	−0·01
Lateral rate of strain Max	0	−0·10	+0·01

TABLE 2. L_u is the integral scale of the turbulence, l_0^2 is the variance of the velocity distribution. Sources of the material are: for the wake, Grant (1958) and Townsend (1956); for the plane jet, Bradbury (1965); for the boundary layer Corrsin & Kistler (1954)

of entrainment velocity to scale velocity is closely related to the entrainment constant defined by

$$\beta = \frac{U_1 + \frac{1}{2}U_m}{\frac{1}{2}U_m}\frac{d\eta_0}{dx}, \tag{8.1}$$

where U_m is the difference between the velocity at the centre of the flow and U_1 the velocity of the ambient fluid. A basic problem for any theory of free turbulence is predicting the entrainment constant for a given kind of flow. As a guide, it is useful to consider the information contained in table 2, which compares in non-dimensional form a number of flow parameters for three kinds of two-dimensional flow, wakes, jets and boundary layers without longitudinal pressure gradient.

Gartshore (1966) has shown a close correlation between the entrainment constant and σ/η_0 the relative depth of the indentations, using observations for a wide variety of free turbulent flows, and the tabulated values illustrate this. It may be noticed that the variations of turbulent intensity and entrainment constant are correlated, roughly with $\beta \propto \overline{q^2}/U_m^2$. A first attempt to explain the difference between the entrainment constants in jets and in wakes supposed that lateral compression of the large eddies in a jet would reduce their size with a consequent reduction in entrainment efficiency (Townsend 1956). The explanation fails to account for the even smaller entrainment constant in a boundary

layer where the lateral compression is negative. Although the flow in a boundary layer differs in important respects from that in jets and wakes, the discrepancy is too great to allow the hypothesis that lateral compression is the cause of the variation. On the other hand, lateral extent of the large eddies is clearly of great importance for determining the rate of entrainment. Here it will be argued that the variations of entrainment constant are primary, in the sense that they are dependent on differences of flow geometry, and that the form of the large eddies is adjusted to produce the required entrainment rate.

First, the environment of the turbulent flow is very similar in wakes and jets, and, to a less extent, in boundary layers. In each flow, the turbulence is confined within bounding surfaces which are not very irregular and is acted on by a distribution of mean velocity which is nearly of the form

$$U = U_1 + U_m \exp(-\tfrac{1}{2}y^2/l_0^2) \tag{8.2}$$

for both wakes and jets. Table 2 shows that the scale of the velocity distribution l_0 is nearly a universal fraction of η_0. For fully developed flow, it is plausible that the turbulent motion should be geometrically similar and characterized by a length scale which is a universal fraction of η_0 and a velocity scale that depends on the flow. The observed values of the integral scale offer some confirmation of the hypothesis. It follows that the total rate of energy dissipation across a half-section of the flow has an average value of

$$\epsilon\eta_0 = (\overline{q^2})_0^{\frac{3}{2}}\eta_0/L, \tag{8.3}$$

where $(\overline{q^2})_0$ is the turbulent intensity at the centre and L is a suitably chosen scale of the turbulent motion.

Another expression for the energy dissipation is the energy equation

$$\epsilon\eta_0 = -\tau_0 U_m + [\overline{pv} + \tfrac{1}{2}\overline{q^2 v}]_0 - \frac{d}{dx}\int_0^\infty \tfrac{1}{2}U[U-U_1)^2 + \overline{q^2}]\,dy \tag{8.4}$$

to the usual 'boundary-layer' approximation, where τ_0 is the shear stress at $y = 0$, and $[\overline{pv} + \frac{1}{2}\overline{q^2 v}]_0$ is the flux of turbulent energy at $y = 0$. For wakes and jets, the first two terms are zero and, assuming that $\overline{q^2} = (\overline{q^2})_0$ for $y < \eta_0$ and is zero for $y > \eta_0$, the integrals can be found for the velocity distribution (8.2). After making use of the conditions for conservation of momentum, $U_m\eta_0 = \text{const.}$ for a wake ($|U_m| \ll U_1$) and $U_m^2\eta_0 = \text{const.}$ for a jet ($U_1 = 0$), we find

$$\epsilon\eta_0 = \frac{\pi^{\frac{1}{2}}}{8} U_m^3 \beta \frac{l_0}{\eta_0}\left[1 + \frac{2}{\pi^{\frac{1}{2}}}\frac{\eta_0}{l_0}\frac{\overline{q^2}}{U_m^2}\right], \tag{8.5W}$$

for a wake, and

$$\epsilon\eta_0 = \frac{1}{4}\left(\frac{\pi}{6}\right)^{\frac{1}{2}} U_m^3 \beta \frac{l_0}{\eta_0}\left[1 + 3^{\frac{1}{2}}\frac{\overline{q^2}}{U_m^2}\right], \tag{8.5J}$$

for a jet. The similarity of boundary layers to wakes and jets extends only to the outer part of the flow beyond the equilibrium, constant-stress layer. Using as the velocity distribution in the outer layer

$$U = U_1 - \left(\frac{2}{\pi}\right)^{\frac{1}{2}} U_m \int_{\alpha y/\eta_0}^\infty e^{-\frac{1}{2}t^2}\,dt, \tag{8.6B}$$

which with $a = 1{\cdot}75$ gives a good description (Townsend 1956), and neglecting the turbulent flux of energy near $y = 0$,†

$$\epsilon\eta_0 = (2\pi^{\frac{1}{2}}a)^{-1}\, U_m^3\beta[1 - \tfrac{1}{2}\pi^{\frac{1}{2}}a\overline{q^2}/U_m^2]. \tag{8.5B}$$

It is assumed that the Reynolds number is very large and use has been made of the momentum equation

$$\tau_0 = \frac{d}{dx}\int_0^\infty U(U_1 - U)\,dy.$$

Geometrical similarity of the turbulence has been assumed and so the ratio of the maximum Reynolds stress to the turbulent intensity is independent of the flow. For a wake, use of the Reynolds equation for the mean flow

$$U\frac{\partial U}{\partial x} + V\frac{\partial U}{\partial y} = -\frac{\partial \overline{uv}}{\partial y},$$

with the velocity distribution (8.2) leads to

$$(-\overline{uv})_m = \tfrac{1}{2}\, e^{-\frac{1}{2}}\, l_0/\eta_0\, U_m^2\beta, \tag{8.7W–J}$$

which is nearly true for a jet. For a boundary layer

$$(-\overline{uv})_m = (2\pi)^{-\frac{1}{2}}a^{-1}U_m^2\beta. \tag{8.7B}$$

Combining (8.3), (8.5) and (8.7) for each flow, we have

$$\beta = \frac{\pi}{8}e^{\frac{3}{2}}\left(\frac{|\overline{uv}|_m}{\overline{q^2}}\right)^3\frac{\eta_0}{l_0}\left(\frac{L}{\eta_0}\right)^2\left[1 + \frac{1}{(\pi e)^{\frac{1}{2}}}\frac{\overline{q^2}}{|\overline{uv}|_m}\beta\right]^2 \tag{8.8W}$$

for a wake,

$$\beta = \frac{\pi}{12}e^{\frac{3}{2}}\left(\frac{|\overline{uv}|_m}{\overline{q^2}}\right)^3\frac{\eta_0}{l_0}\left(\frac{L}{\eta_0}\right)^2\left[1 + \left(\frac{3}{4e}\right)^{\frac{1}{2}}\frac{\overline{q^2}}{|uv|_m}\frac{l_0}{\eta_0}\beta\right]^2 \tag{8.8J}$$

for a jet, and

$$\beta = \frac{\pi^{\frac{1}{2}}a}{2^{\frac{1}{2}}}\left(\frac{|\overline{uv}|_m}{\overline{q^2}}\right)^3\left(\frac{L}{\eta_0}\right)^2\left[1 - \frac{1}{2\sqrt{2}}\frac{\overline{q^2}}{|\overline{uv}|_m}\beta\right]^2 \tag{8.8B}$$

for a boundary layer.

The expressions for the entrainment constant involve three universal constants, $\overline{q^2}/|\overline{uv}|_m$, L/η_0 and η_0/l_0 (or a for a boundary layer), whose values can be chosen within limits. After a large plane strain, homogeneous turbulence develops a value of $\overline{q^2}/|\overline{uv}|$ near 6 (Townsend 1956), but smaller values are common in free turbulent flows (table 1). In grid turbulence (Batchelor 1953), the scale L is approximately three times the integral scale of the turbulence, which is of order $\frac{1}{2}\eta_0$ (table 1). The mean position of the bounding surface must be just within the range of mean velocity variation, a condition that implies a value of η_0/l_0 near 2. To fit the wake observations, we use the observed values

$$\overline{q^2}/|\overline{uv}|_m = 3{\cdot}5, \quad \eta_0/l_0 = 2{\cdot}0, \quad \beta = 0{\cdot}40$$

to show that $L/\eta_0 = 1{\cdot}49$. Substituting in (8.8J) and (8.8B), entrainment constants for jets and boundary layers are found, in fair agreement with

† It is at most of order $(\overline{q^2})^{\frac{3}{2}}$ and less than (say) $\tau_0 U_m$ in a ratio $(\overline{q^2})^{\frac{1}{2}}/U_m$.

observation for the jet (see table 3). (For a boundary layer, $a = 1{\cdot}75$ is equivalent to a value of η_0/l_0 of 2.)

It appears that the variation of entrainment constant between wakes and jets can be explained on the assumption of geometrical similarity of the turbulent motion within the bounding surfaces without any detailed consideration of the process of entrainment. The stability considerations of the previous section indicate that the indentations are in the form of wave groups with wave-number rather less than k_0, the wave-number for critical stability, which satisfies the condition (see (7.3))

$$\epsilon k_0^{-1} = A^3 V^3(k_0), \tag{8.9}$$

where $V(k_0)$ is the effective relative velocity. Combining the stability condition with (8.7),

$$\beta = 2e^{\frac{1}{2}} A^2 \frac{|\overline{uv}|_m}{\overline{q^2}} \frac{\eta_0}{l_0} \left(\frac{L}{\eta_0}\right)^{\frac{2}{3}} (k_0\eta_0)^{\frac{2}{3}} (V(k_0)/U_m)^2 \tag{8.10 W–J}$$

for wakes and jets, and

$$\beta = (2\pi)^{\frac{1}{2}} A^2 (|\overline{uv}|_m/\overline{q^2}) (L/\eta_0)^{\frac{2}{3}} (k_0\eta_0)^{\frac{2}{3}} [V(k)/U_m]^2 \tag{8.10B}$$

	Wake		Jet		Boundary layer	
Quantity	Observed	Theory	Observed	Theory	Observed	Theory
β	0·40	0·40*	0·18	0·16	0·048	0·09
$\bar{k}\eta_0$	2	2*	3·1	3·4	2·6	2·5 (3.6)
σ/η_0	0·38	0·4*	0·22	0·26	0·17	0·32 (0·22)
$\overline{q^2}/U_m^2$	0·21	0·21*	0·13	0·085	0·08	0·072 (0·038)

TABLE 3. (*a*) Asterisks indicate that the various constants have been selected to produce the 'theoretical' value. (*b*) The bracketed values for the boundary layer have been calculated using the observed value of β, i.e. not using the energy equation (8·5B). (*c*) It is assumed that $\bar{k}\eta_0 = 0{\cdot}6\, k_0\eta_0$ and that $\bar{k}\sigma = 0{\cdot}8$

for boundary layers. Changing the definition of entrainment constant for a boundary layer to

$$\beta' = (2/\pi)^{\frac{1}{2}} a^{-1} (\eta_0/l_0)\, 2e^{\frac{1}{2}} \beta, \tag{8.11}$$

the equations become identical. Figure 7 shows the predicted variation of $(k_0\eta_0)^{-1}$ with β, assuming that

$$V(k_0) = U(\eta_0 - 2k_0^{-1}) \tag{8.12}$$

and that $A = 0{\cdot}359$, chosen to agree with the wake values, $(k_0\eta_0)^{-1} = 0{\cdot}3$, $\beta = 0{\cdot}40$. The dominant wave-number of the wave groups is expected to be rather less than k_0, and, since surface slopes of order one are the prelude to engulfment and the end of an entrainment cycle, the average depth of the indentations is about k_0^{-1}.

Observed and predicted values of β, $\bar{k}\eta_0$ ($\bar{k}$, the dominant wave-number of a group, is assumed to be $0{\cdot}6k_0$), $\overline{q^2}/U_m^2$ and σ/η_0 are listed in table 3 for the three flows. Reasonable agreement is found between the values for wakes and jets

but the boundary-layer predictions are less good. In view of the substantial differences in the environment of the turbulent flow, notably the presence of the wall instead of a plane of symmetry, no better agreement could be expected.

9. Influence of flow density on entrainment rate

By supposing that the growth of indentations of the bounding surface is controlled by an instability mechanism dependent on elastic behaviour of the turbulent fluid, most of the observed features of the large eddies can be explained, but the considerations of the previous section show that the bulk properties of

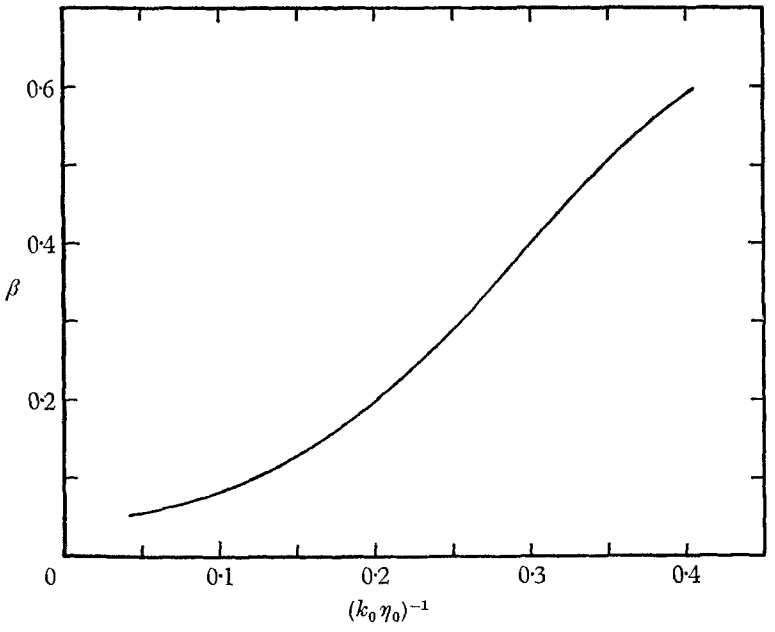

FIGURE 7. Dependence of critical wave-number on entrainment constant for jets and wakes.

the flow do not depend critically on the exact mechanism of the entrainment. The arguments used there assume geometrical similarity of the turbulent motion in the different flows, which is possible if the energy released directly by the individual engulfments is nearly in proportion to that released by working of the velocity gradient against the Reynolds stresses in the interior of the turbulent fluid. If the density of the turbulent fluid differs greatly from that of the ambient fluid, conditions in the entrainment layer, say within a distance σ of the mean position of the bounding surface, are probably very different from those in the interior. Then the actual mechanism of the entrainment becomes important and it might be possible to distinguish between different mechanisms by measuring the variation of entrainment constant with density ratio.

Consider a circular jet of one fluid entering and mixing with another of different density, and assume that the distributions of mean velocity and density

difference are similar in form at all sections of the jet. Then the fluxes of momentum and of density defect

$$M = 2\pi \int_0^\infty \rho U^2 r\, dr \quad \text{and} \quad Q = 2\pi \int_0^\infty (\rho_a - \rho)\, U r dr$$

are independent of distance from the jet orifice, and provide two relations between the effective radius of the flow η_0, the maximum velocity U_m, and the maximum density difference $\rho_a - \rho_m$. If the density defect is small, the development of the jet can be calculated, since the rate of increase of flow radius is determined by the velocity and length scales and by the properties of the fluid. Since viscosity has no direct influence on fully turbulent flow, the entrainment constant is a function of the local density ratio, ρ_m/ρ_a, which is nearly one at all distances from the flow origin for small density differences.

The equilibrium hypothesis supposes that the bounding surface develops indentations that grow and engulf ambient fluid, and that are controlled by a mechanism keeping them near a condition of critical stability. For elastic behaviour of the turbulent fluid and appreciable density difference, (6.2) can be modified to give the phase velocity of a surface wave as $c - V$, where c satisfies

$$\rho_a (c - V)^2 = \bar{\rho}(n^2/c^2)\,[4(1 - c^2/n)^{\frac{1}{2}} - (2 - c^2/n)^2], \tag{9.1}$$

where V is the effective velocity of the turbulent fluid and $\bar{\rho}$ is the effective density. Both V and $\bar{\rho}$ should be evaluated at a depth of order k^{-1} within the turbulent fluid. For marginal stability, the equation has equal roots and it is not difficult to show that the critical value of $V - c$, the phase velocity relative to the ambient fluid, is nearly $V\bar{\rho}/(\rho_a + \bar{\rho})$ for any density ratio. The spreading of the flow depends on the growth of indentations to a large amplitude during the unstable phase of a growth–decay cycle and we require the growth rate when the rigidity is rather less than the critical value. The instability is of the Helmholtz type so that the logarithmic growth rate is about $kV(\rho_a\bar{\rho})^{\frac{1}{2}}/(\rho_a + \bar{\rho})$ (Lamb 1932), the indentations travelling with velocity $V\bar{\rho}/(\rho_a + \bar{\rho})$ in agreement with the phase velocity of the critically stable waves. Then the logarithm of the amplification ratio is

$$\alpha = kV\tau(\rho_a\bar{\rho})^{\frac{1}{2}}\,(\rho_a + \bar{\rho}), \tag{9.2}$$

where τ is the time available for growth, perhaps about half the time necessary for a complete growth–decay cycle. In the time for a complete cycle, the wave crests extend out a distance of order k^{-1} and the wave group travels a distance of order $V\tau\bar{\rho}/(\rho_a + \bar{\rho})$. It follows that the rate of increase of flow width is proportional to the ratio of k^{-1} to the distance travelled by the wave group, i.e.

$$d\eta_0/dx = (\rho_a/\bar{\rho})^{\frac{1}{2}}\beta_1, \tag{9.3}$$

since α is not expected to vary much from one flow to another. β_1 is the entrainment constant for no density difference.

If the controlling influence is eddy viscosity, the condition that a disturbance of amplitude a_0, of wave-number k and travelling with phase velocity $c - V$, should have its growth rate considerably retarded by the viscosity, is of the form

$$ka_0[\rho_a(c - V)^2 + \bar{\rho}c^2] \approx \bar{\rho}\nu_T k^2 a_0 c, \tag{9.4}$$

equating unbalanced pressures at the interface caused by accelerations to Reynolds stresses in the turbulent fluid. The phase velocity relative to the ambient fluid must be near $V\rho_a/(\rho_a+\bar{\rho})$, and so the (kinematic) eddy viscosity required is

$$\nu_T \approx \frac{\rho_a}{\rho_a+\bar{\rho}}\frac{c}{k} = \frac{V}{k}. \tag{9.5}$$

An eddy viscosity of this magnitude for waves with not too large $k_0\eta_0$ is obtained if

$$(\overline{q^2})^{\frac{1}{2}} \approx V. \tag{9.6}$$

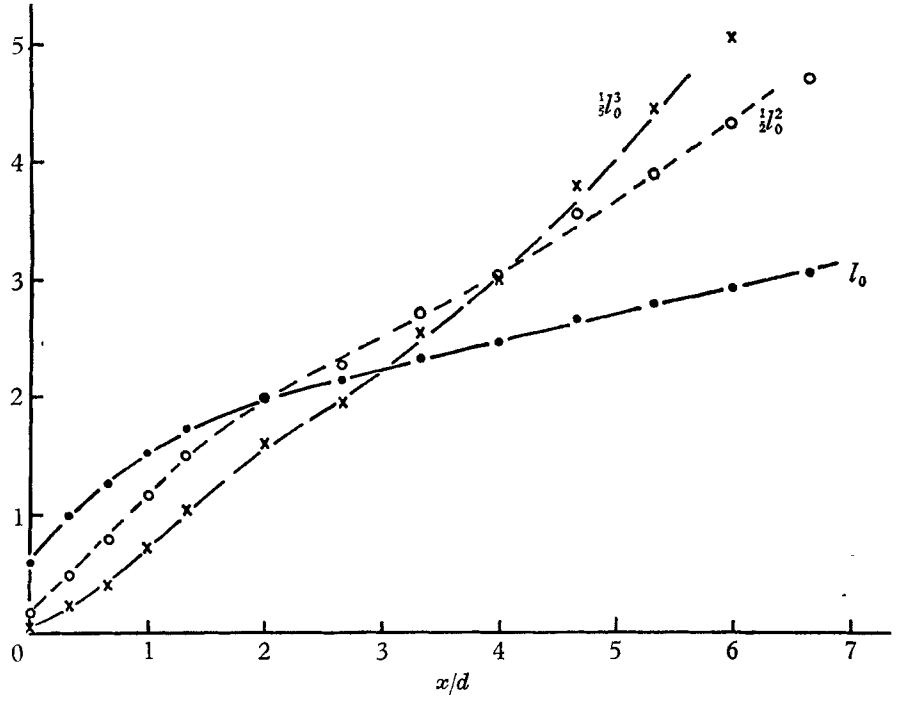

FIGURE 9. Variation of jet width with distance from orifice for a high-speed jet of air entering water. ●, l_0; ○, $\frac{1}{2}l_0^2$; ×, $\frac{1}{5}l_0^3$.

The initial disturbance is derived from the main turbulent motion and has an initial velocity of order $(\overline{q^2})^{\frac{1}{2}}$. The control process prevents excessive growth, and so the indentations must advance into the ambient fluid with a velocity of order $(\overline{q^2})^{\frac{1}{2}}$. Since the phase velocity of the growing indentations is $V\bar{\rho}/(\rho_a+\bar{\rho})$, the rate of spread is

$$\left.\begin{aligned} d\eta_0/dx &\propto V/[V\bar{\rho}/(\rho_a+\bar{\rho})] = (\rho_a+\bar{\rho})/\bar{\rho}, \\ \text{i.e.} \qquad d\eta_0/dx &= \beta_1(\rho_a+\bar{\rho})/2\bar{\rho}. \end{aligned}\right\} \tag{9.7}$$

The variations of entrainment constant with density ratio derived from the two hypotheses of elastic and viscous control are very similar if the densities are within a factor of two, but the elastic hypothesis predicts much smaller rates of spread for very large and very small density ratios. Unfortunately, pairs of miscible fluids of widely different densities are rare and the use of immiscible fluids introduces the complications of surface tension. Supposing that

jets of sufficiently high speed contain locally homogeneous suspensions of one phase in the other, liquid–gas combinations are suitable for a test of the predictions (figure 8, plates 2 and 3). High-speed jets of water in air have quite small angles of spread even when the jet exit is roughened to accelerate the disintegration of the jet (figure 8(*d*)) and this behaviour is consistent only with the elastic model. It is possible, however, that the central visible jet is surrounded by a much thicker air-flow resembling an axisymmetric boundary layer, and the effective velocity of the ambient fluid may be quite large instead of being negligible. The reverse configuration of an air jet issuing into water is not subject to this particular objection but it is doubtful how large an effective density ratio is possible. Figure 8(*a*) (plate 2) shows a photograph of such a jet. Use of the conservation equations and the two entrainment equations (9.3) and (9.7) show that for large values of $\rho_a/\overline{\rho}$, $\eta_0 \propto (x-x_0)^{\frac{1}{2}}$ for elastic control and that $\eta_0 \propto (x-x_0)^{\frac{1}{3}}$ for viscous control. The squares and cubes of the flow widths are plotted against axial distance in figure 9 and slightly better agreement is found with the elastic prediction, but the evidence is not decisive.

10. Concluding remarks

It has been shown that many of the observed features of the entrainment process can be explained if the large eddies are controlled by elastic behaviour of the turbulent fluid. The particular consequences of elastic behaviour arise from the stability of the shorter wavelengths of surface indentation, so that folding is confined to moderately large scales and the surface remains sharp to within the Kolmogoroff length scale. Further, the fast-growing indentations are limited to a narrow range of wave-numbers and the typical amplified disturbance is a group of about three waves. Reasonable numerical agreement with the observations is obtained with the simple flow model used here, but it might be useful to consider in more detail the stability problem with a continuous distribution of velocity within the turbulent fluid. Most existing knowledge of the characteristics of the bounding surface has been obtained indirectly and more direct and extensive studies of the surface would reduce the need for speculation in theories of entrainment. The most valuable measurements would be of the space–time spectra of the surface displacement which would allow determination of the phase velocities of the indentations and of the dominant wavelengths.

Appendix: waves on the interfaces between a layer of turbulent fluid and the surrounding inviscid stream

Consider a layer of turbulent fluid initially bounded by the planes $y = \pm h$, and with zero mean velocity in the co-ordinate system. Surrounding it is an inviscid, irrotational stream moving with velocity V in the Ox-direction, and we wish to investigate the propagation and growth of waves of small amplitude. Since the component of stream velocity parallel to the wave fronts has no influence on the motion, it is sufficient to consider only waves with fronts normal to the Ox-direction. Entrainment is neglected so there is a sharp distinction between turbulent and irrotational fluid.

If the surface displacement at the boundary is

$$\eta(h) = \eta_0(h) \exp ik(x-ct), \tag{A 1}$$

where c may be complex, the theory of potential flow shows that the pressures at the boundary are given by

$$p(h) = -k(c-V)^2 \eta(h). \tag{A 2}$$

The motion of the turbulent fluid must be able to satisfy the appropriate equations of motion and to cause zero shear stress and normal stresses given by (A 2) at the boundaries. If the turbulent fluid behaves as a Newtonian fluid of kinematic viscosity ν, the equation of motion for small velocities is

$$\partial \mathbf{u}/\partial t = -\operatorname{grad} p + \nu \nabla^2 \mathbf{u}. \tag{A 3}$$

If it behaves as an incompressible elastic jelly of kinematic rigidity n, the equation of motion for small particle displacements $\boldsymbol{\xi}$ is

$$\partial^2 \boldsymbol{\xi}/\partial t^2 = -\operatorname{grad} p + n \nabla^2 \boldsymbol{\xi}. \tag{A 4}$$

In both cases the turbulent fluid is incompressible and taking the divergence of the equations of motion leads to an equation for the pressure,

$$\nabla^2 p = 0, \tag{A 5}$$

whose solution is

$$p = (p_a \sinh ky + p_s \cosh ky) \exp ik(x-ct). \tag{A 6}$$

The two terms refer to antisymmetric and symmetric modes of boundary displacement. Except for the necessity of interchanging hyperbolic sines with hyperbolic cosines, the analysis is the same for each mode.

First, consider the antisymmetric mode with viscous behaviour of the turbulent fluid. Introducing the stream function,

$$\psi = \psi_0(y) \exp ik(x-ct).$$

such that $u = \partial\psi/\partial y$, $v = -\partial\psi/\partial x$, the equation of motion (A 3) becomes

$$\psi_0'' - k^2[1-(ic/\nu k)]\,\psi_0 = (ip_a/\nu)\cosh ky, \tag{A 7}$$

after a little rearrangement. The boundary conditions are that the shear stress, $\nu[(\partial u/\partial y + (\partial v/\partial x)]$, is zero on both bounding surfaces, $y = \pm h$, and the appropriate solution is

$$\psi_0 = \frac{p_a}{kc}\left[\cosh ky - \frac{2}{2-ic/\nu k}\frac{\cosh kh}{\cosh k'h}\cosh k'y\right], \tag{A 8}$$

where $k' = k[1-ic/(k\nu)]^{\frac{1}{2}}$. The other conditions are that normal stresses are continuous across the bounding surface and that the velocity field on each side should produce the same distortion. The normal stress inside the turbulent fluid is $p - 2\nu\partial v/\partial y$ and is equal to $p(h)$. So

$$p(h) = p_a\left[\left(1+\frac{2i\nu k}{c}\right)\sinh kh - \frac{4i\nu k/c}{2-ic/\nu k}\frac{k'}{k}\frac{\cosh kh}{\cosh k'h}\sinh k'h\right]. \tag{A 9}$$

Since the rate of change of $\eta(h)$ following the turbulent fluid is $v = -ik\psi$, $\psi_0(h) = c\eta_0(h)$, (A 2) and (A 9) lead to

$$\left(\frac{c-V}{\nu k}\right)^2 = \left(2-\frac{ic}{\nu k}\right)^2 \tanh kh - 4\left(1-\frac{ic}{\nu k}\right)^{\frac{1}{2}} \tanh k'h, \tag{A 10}$$

a relation between the complex phase velocity, the wave-number and the relative velocity. For large values of kh, it reduces to

$$\left(\frac{c-V}{\nu k}\right)^2 = \left(2-\frac{ic}{\nu k}\right)^2 - 4\left(1-\frac{ic}{\nu k}\right)^{\frac{1}{2}}. \tag{A 11}$$

For small values of kh, it becomes

$$(c-V)^2 = -khc^2, \tag{A 12}$$

leading to

$$c = V(1+i(kh)^{\frac{1}{2}}), \tag{A 13}$$

indicating a logarithmic growth rate of $(kh)^{\frac{1}{2}}kV$. With large values of kh, (A 11) leads to

$$c = \tfrac{1}{2}iV^2/(\nu k), \tag{A 14}$$

if the Reynolds number $c/(\nu k)$ is small, and to the well-known result for a vortex sheet,

$$c = \tfrac{1}{2}V(1+i), \tag{A 15}$$

if the Reynolds number is large.

For turbulent fluid which behaves as an incompressible jelly, the displacements are conveniently described by a function,

$$\phi = \phi_0(y) \exp ik(x-ct),$$

such that the Ox- and Oy-components of the displacement are $\xi = \partial\phi/\partial y$ and $\eta = -\partial\phi/\partial x$. Substituting the antisymmetric pressure distribution in the equation of motion (A 4), we obtain

$$\phi_0'' - k^2(1-c^2/n)\,\phi_0 = i(p_a/n)\cosh ky, \tag{A 16}$$

and, after applying the boundary condition of zero shear stress at $y = \pm h$, the solution is found to be

$$\phi_0(y) = \frac{ip_0}{k^2c^2}\left[\cosh ky - \frac{2}{2-c^2/n}\frac{\cosh kh}{\cosh [kh(1-c^2/n)^{\frac{1}{2}}]}\cosh [ky(1-c^2/n)^{\frac{1}{2}}]\right]. \tag{A 17}$$

The normal stress inside the turbulent jelly is $-p + 2n\,\partial\eta/\partial y$ and so the pressure just outside the bounding surface is

$$p(h) = -p_0 \cosh kh\left[\left(\frac{2n}{c^2}-1\right)\tanh kh - \frac{4n}{c^2}\frac{(1-c^2/n)^{\frac{1}{2}}}{2-c^2/n}\tanh [kh(1-c^2/n)^{\frac{1}{2}}]\right]. \tag{A 18}$$

Equating to the pressure in the inviscid fluid, we obtain a relation analogous to (A 10),

$$\frac{(c-V)^2}{n} = \frac{n}{c^2}[4(1-c^2/n)^{\frac{1}{2}} \tanh \{kh(1-c^2/n)^{\frac{1}{2}}\} - (2-c^2/n)^2 \tanh kh]. \tag{A 19}$$

For large values of kh, it becomes

$$(c-V)^2/n = (n/c^2)\,[4(1-c^2/n)^{\frac{1}{2}} - (2-c^2/n)^2], \tag{A 20}$$

and it is identical with the relation for viscous behaviour (A 12) if kh is small. Considered as a function of $c/n^{\frac{1}{2}}$, the right-hand side of the equation has a maximum value of 2 for $c/n^{\frac{1}{2}} = 0$ and decreases steadily to -1 as $c/n^{\frac{1}{2}}$ increases to 1. For larger values of $c/n^{\frac{1}{2}}$, it is complex. The left-hand side has a parabolic variation with the opposite curvature and, for $c/n^{\frac{1}{2}}$ less than 0·63, there are two real roots.† The critical condition with identical real roots occurs for $V = 1{\cdot}79n^{\frac{1}{2}}$ and a phase velocity relative to the inviscid fluid of $V - c = 1{\cdot}16n^{\frac{1}{2}}$. With smaller values of kh, the variation of the right-hand side is similar but less in magnitude for antisymmetrical disturbances. If the disturbances are symmetrical, the tanh functions in (A 19) become coth functions and the magnitudes are greater if kh is smaller. The result is that antisymmetrical disturbances become unstable at smaller values of the difference velocity than symmetrical disturbances of the same wave-number.

REFERENCES

Batchelor, G. K. 1953 *The Theory of Homogeneous Turbulence.* Cambridge University Press.

Bradbury, L. J. S. 1965 *J. Fluid Mech.* **23**, 31.

Bradshaw, P., Ferriss, D. H. & Johnson, R. F. 1964 *J. Fluid Mech.* **19**, 591.

Clauser, F. H. 1956 *Adv. Appl. Mech.* **4**, 1.

Corrsin, S. 1943 *Nat. Adv. Comm. Aero., Wash., Wartime Rept* no. 94.

Corrsin, S. & Kistler, A. L. 1954 *Nat. Adv. Comm. Aero., Wash., TN* no. 3133.

Davies, P. O. A. L. 1964 Private communication.

Franklin, R. E. & Foxwell, J. H. 1958*a* *Aero. Res. Counc. (London) R. & M.* no. 3161.

Franklin, R. E. & Foxwell, J. H. 1958*b* *Aero. Res. Counc. (London) R. & M.* no. 3162.

Gartshore, I. S. 1966 *J. Fluid Mech.* **24**, 89.

Grant, H. L. 1958 *J. Fluid Mech.* **4**, 149.

Keffer, J. F. 1965 *J. Fluid Mech.* **22**, 135.

Klebanoff, P. S. 1954 *Nat. Adv. Comm. Aero., TN* no. 3178.

Lamb, H. 1932 *Hydrodynamics.* Cambridge University Press.

Lin, C. C. 1959 *Turbulent Flows and Heat Transfer.* Oxford University Press.

Phillips, O. M. 1955 *Proc. Camb. Phil. Soc.* **51**, 220.

Reynolds, A. J. 1962 *J. Fluid Mech.* **13**, 333.

Townsend, A. A. 1949 *Australian J. Sci. Res.* **2**, 451.

Townsend, A. A. 1951 *Phil. Mag.* **41**, 890.

Townsend, A. A. 1954 *Quart. J. Mech. Appl. Math.* **4**, 308.

Townsend, A. A. 1956 *The Structure of Turbulent Shear Flow.* Cambridge University Press.

Wills, J. A. B. 1964 *J. Fluid Mech.* **20**, 417.

† (A 20) can be rationalized into a sextic equation for c, and it might appear that there are two conjugate pairs of complex roots besides the two real ones. Because (A 20) is derived from (A 19) as the limit for $|(1-c^2/n)^{\frac{1}{2}}\, kh| \to \infty$, the only possible value of $(1-c^2/n)^{\frac{1}{2}}$ is one with a positive real part. For specific values of V, it can be shown that the complex roots satisfy the original equation only if $(1-c^2/n)^{\frac{1}{2}}$ is chosen with a negative real part. A physical argument is that no source of energy exists if $V = 0$ and that there are then only two real roots, corresponding to the two possible directions of propagation. If V is allowed to increase, the appearance of additional roots is to be expected only if new kinds of motion become possible.